

**Contract No:**

This document was prepared in conjunction with work accomplished under Contract No. DE-AC09-08SR22470 with the U.S. Department of Energy (DOE) Office of Environmental Management (EM).

**Disclaimer:**

This work was prepared under an agreement with and funded by the U.S. Government. Neither the U. S. Government or its employees, nor any of its contractors, subcontractors or their employees, makes any express or implied:

- 1 ) warranty or assumes any legal liability for the accuracy, completeness, or for the use or results of such use of any information, product, or process disclosed; or
- 2 ) representation that such use or results of such use would not infringe privately owned rights; or
- 3) endorsement or recommendation of any specifically identified commercial product, process, or service.

Any views and opinions of authors expressed in this work do not necessarily state or reflect those of the United States Government, or its contractors, or subcontractors.

# $\beta$ -Ga<sub>2</sub>O<sub>3</sub> for Next Generation X-ray Detectors

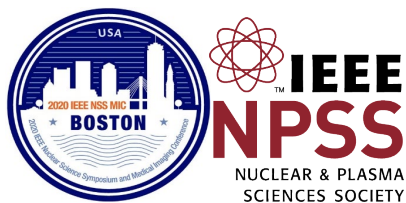
Ibrahim Hany, Ge Yang\*

North Carolina State University, Raleigh, NC, 27695-7909, USA

(\*Email: gyang9@ncsu.edu)

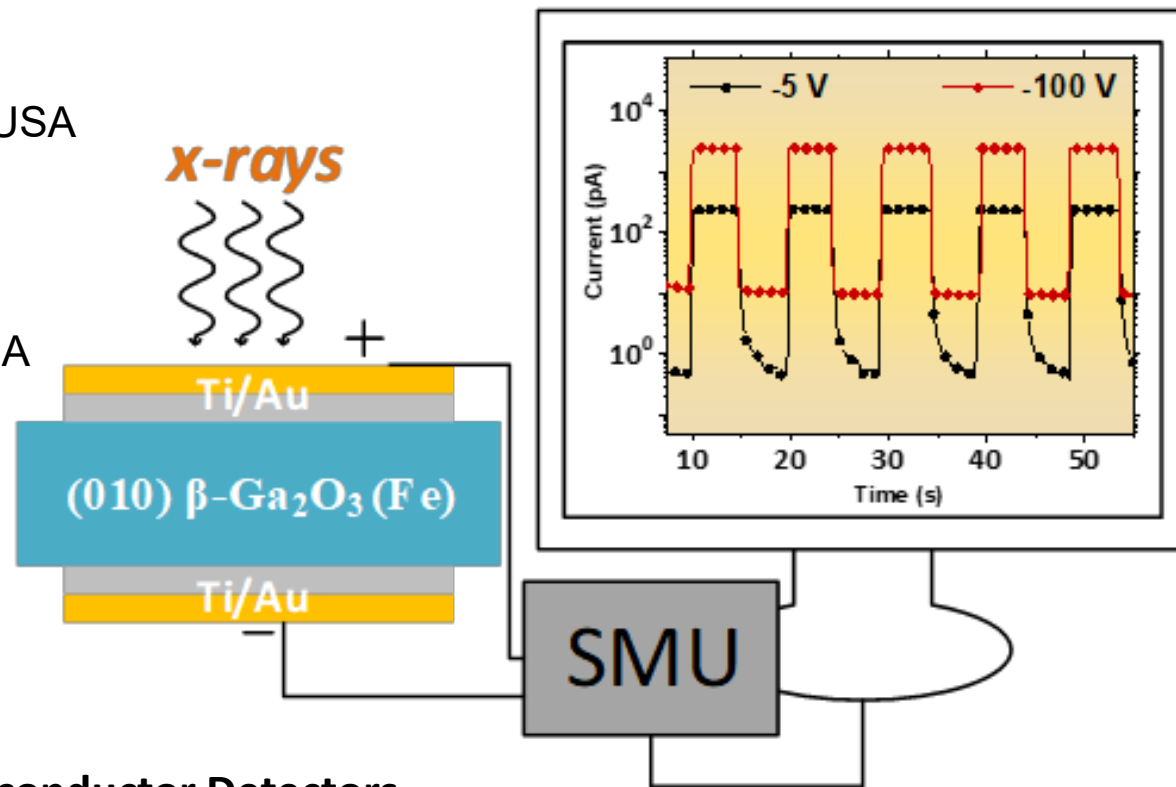
Ralph B. James

Savannah River National Laboratory, Aiken, SC, 29808, USA



2020 IEEE NSS & MIC

27<sup>th</sup> International Symposium on Room-Temperature Semiconductor Detectors

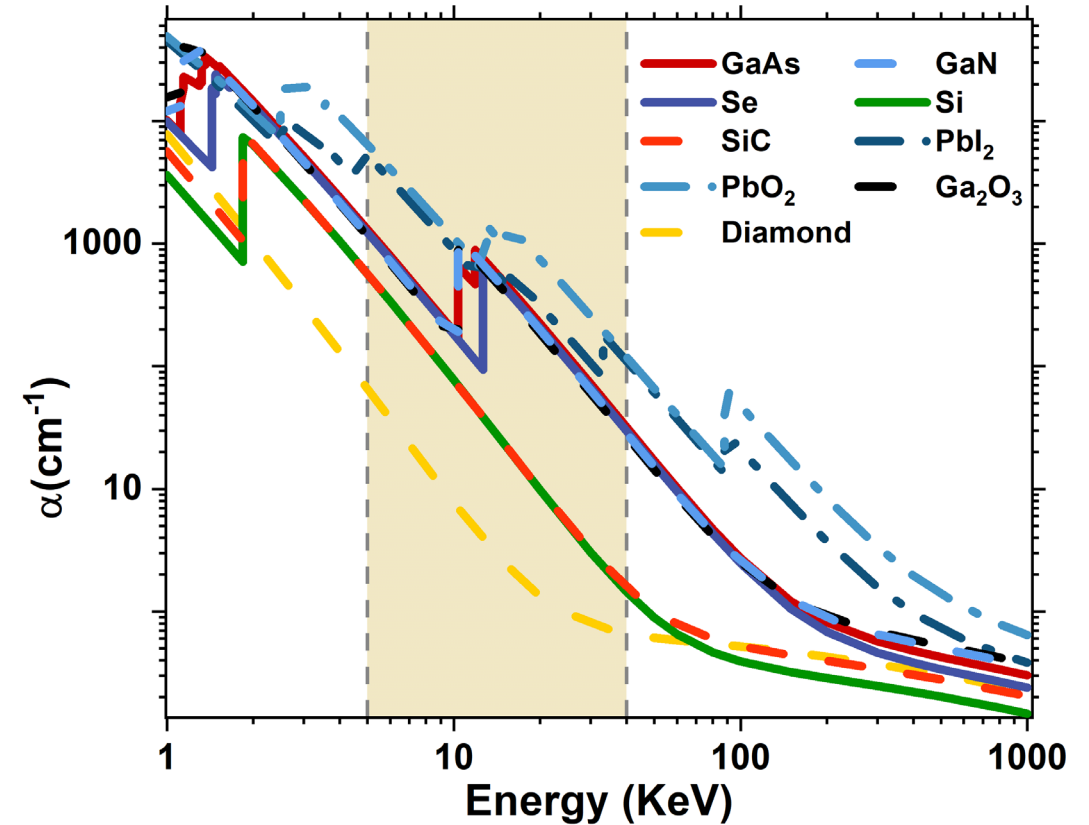


# Outline

- I. Motivation
- II. Introduction
- III. Optical and electrical characteristics of  $\beta$ -Ga<sub>2</sub>O<sub>3</sub> (Fe)
- IV. X-ray Induced Current (XRIC) Characterization
- V. Temperature-dependent Cathodoluminescence (CL) for  $\beta$ -Ga<sub>2</sub>O<sub>3</sub> (Fe)
- VI. Summary

# I. Motivation – the need for (U)WBG detectors

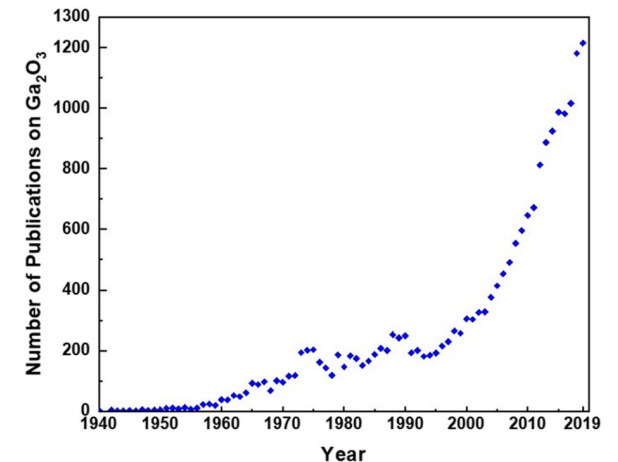
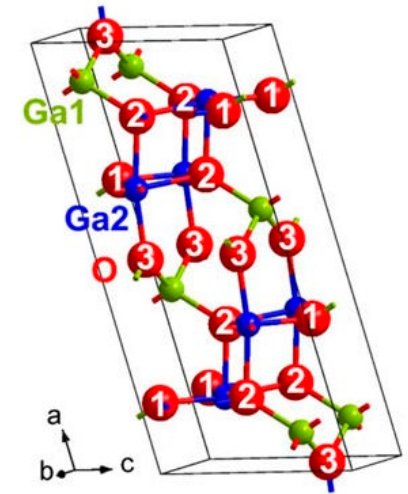
- Radiation detectors are key components for numerous products and applications.
- Elementary detectors have many limitations related to their intrinsic material properties.
  - Harsh environment
  - Cooling and compromised density
  - High Voltage operation
- Wide and ultrawide bandgap semiconductors are much less susceptible to displacement damage by particle irradiation than elemental and narrow bandgap compound semiconductors.



I. Hany et al., "Fast X-ray detectors based on bulk  $\beta$ -Ga<sub>2</sub>O<sub>3</sub> (Fe)," J. Mater. Sci. 55, 9461-9469, 2020.

# I. Motivation – Ga<sub>2</sub>O<sub>3</sub> for radiation detection

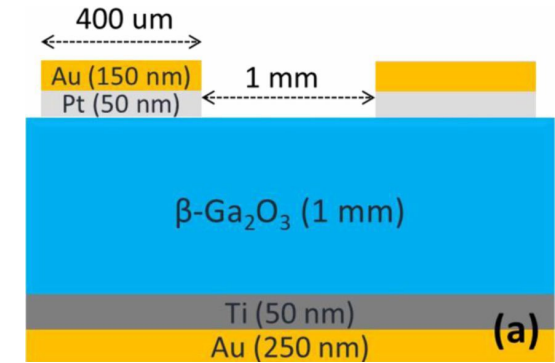
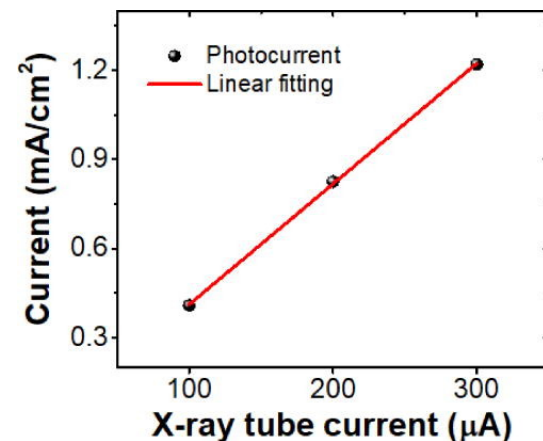
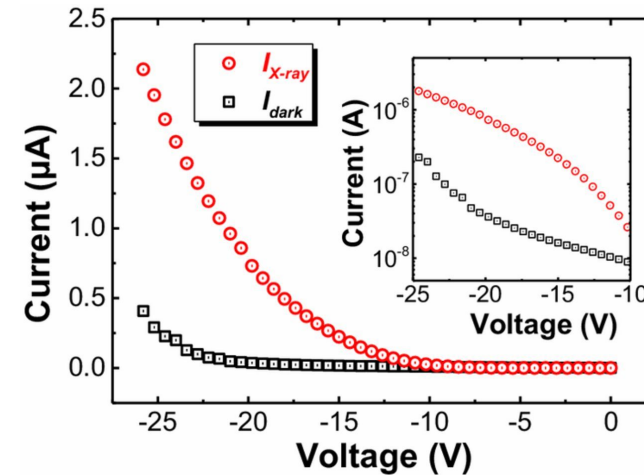
- **β-Ga<sub>2</sub>O<sub>3</sub> has many material advantages**
  - Thermal stability (M. P. > 1800 °C)
  - The least mature and most recent ultrawide bandgap material (4.5 – 5.1 eV)
  - Very high breakdown electric field (8 MV/m)
  - Control of n-type conductivity via doping and post-growth processes
  - High-quality bulk single crystals from melt
  - Cost-effective large-scale manufacturability
- **β-Ga<sub>2</sub>O<sub>3</sub> holds high promise for addressing many radiation detection application needs not met by currently used materials**
  - Harsh environment applicability
  - Versatile and cost-effective synthesis and fabrication
  - High detector performance



J. Zhang et al., "Recent progress on the electronic structure, defect, and doping properties of Ga<sub>2</sub>O<sub>3</sub>," APL Materials, 8, 2, 20906, 2020.

## II. Introduction – X-ray sensors based on $\beta\text{-Ga}_2\text{O}_3$

- One previous study published in 2018-2019
  - Annealed at 1500 °C in air atmosphere for 48 hours
  - Double-side chemical mechanical polishing (CMP)
- Response linearity was demonstrated with no saturation effect.
- High photo-to-dark current ratio exceeding 800 at –15 V.
- When biased at 0V, the detector showed perfect photovoltaic characteristics, demonstrating the great potential of using  $\beta\text{-Ga}_2\text{O}_3$  SBDs as passive X-ray detectors or X-ray photocells.

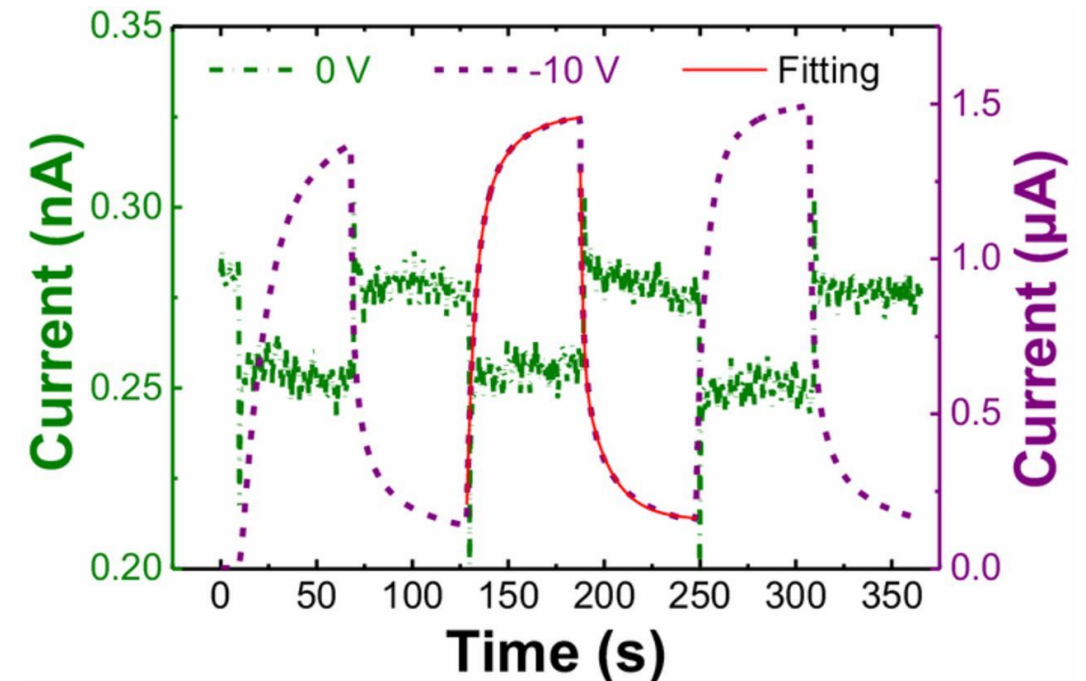


(100) undoped  $\beta\text{-Ga}_2\text{O}_3$  EFG based x-ray sensors

X. Lu et al., "X-ray Detection Performance of Vertical Schottky Photodiodes Based on a Bulk  $\beta\text{-Ga}_2\text{O}_3$  Substrate Grown by an EFG Method," ECS J. Solid State Sci. Technol. 8, 7, Q3046–Q3049, 2019.

## II. Introduction – X-ray sensors based on $\beta\text{-Ga}_2\text{O}_3$

- Two different time constants are obtained for the photocurrent rising process ( $\tau_{r1} = 13.8$  s and  $\tau_{r2} = 1.4$  s), while during the photocurrent decaying process the two time-constants are  $\tau_{d1} = 17.1$  s and  $\tau_{d2} = 4.0$  s.
- The fast response of an unbiased SBD detector corresponds to a photovoltaic mechanism, where the photo-generated carriers in the space-charge region are swept out rapidly by the built-in electric field.

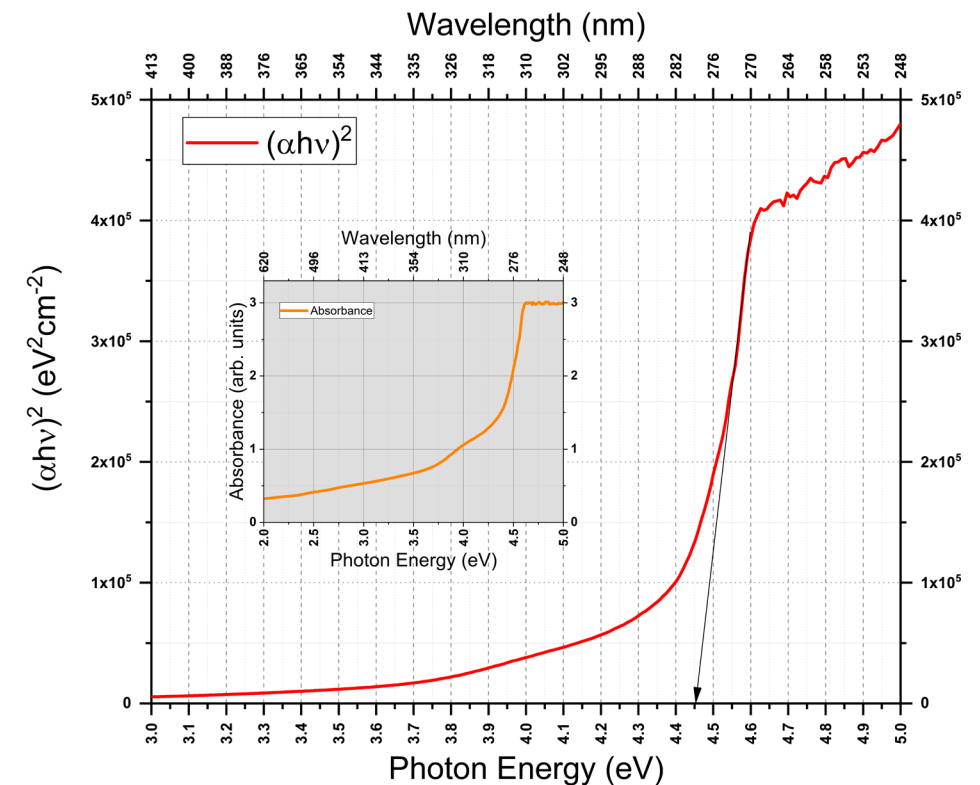


X. Lu et al., "X-ray Detection Performance of Vertical Schottky Photodiodes Based on a Bulk  $\beta\text{-Ga}_2\text{O}_3$  Substrate Grown by an EFG Method," ECS J. Solid State Sci. Technol. 8, 7, Q3046–Q3049, 2019.

### III. Optical and electrical characterization – bandgap

- Optical bandgap deducted from Tauc plot was 4.45 eV based on direct band gap treatment.
- No near band-gap shoulder was shown.
- The UWB opens the path for UV detection and the possibility for x-ray,  $\gamma$ -ray detection as well as charged particles.

Tauc Plot showing optical bandgap of 4.45 eV. Inset shows optical absorption curve raw data which was used for Tauc plot construction.

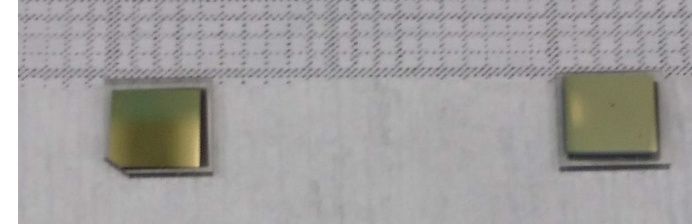


I. Hany et al., "Low temperature cathodoluminescence study of Fe-doped  $\beta$ - $\text{Ga}_2\text{O}_3$ ," Materials Letters 257, 126744, 2019.

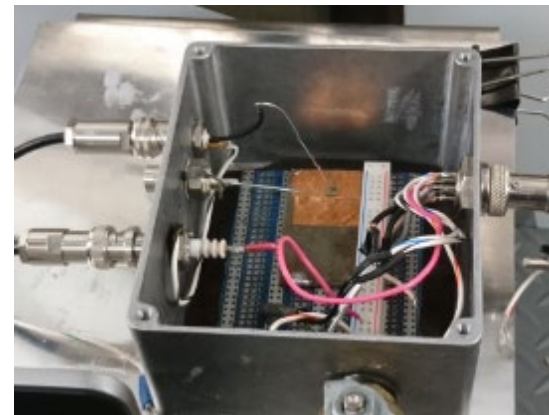


### III. Optical and electrical characterization – resistivity

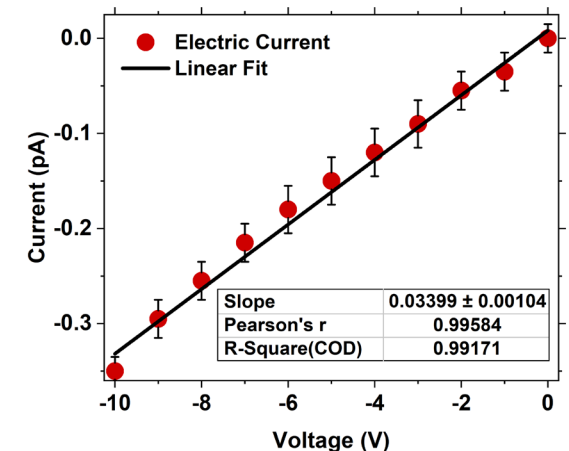
- $4 \times 4 \text{ mm}^2$  Au/Ti (50/50 nm) electrodes were deposited on both sides of  $5 \times 5 \text{ mm}^2$  sample.
  - DC sputtering for Ti, e-beam for Au
- Very high resistivity in the order of  $10^{14} \Omega \cdot \text{cm}$  was revealed from I-V measurement.
- $4 \times 4 \text{ mm}^2$  Au/Ti (50/50 nm) and Au/Ni (40/50 nm) electrodes were deposited for testing Schottky behavior; however the I-V behavior was not different from the Au/Ti Ohmic sample.
  - DC sputtering for Ti, e-beam for Au and Ni
- Controlled 10-minute air annealing at  $400 \text{ }^\circ\text{C}$  didn't change I-V behavior for both samples.



Au/Ni/ $\beta$ -Ga<sub>2</sub>O<sub>3</sub>/Ti/Au and Au/Ti/ $\beta$ -Ga<sub>2</sub>O<sub>3</sub>/Ti/Au



In-house built versatile testing box used for I-V, XRIC and UVIC measurements



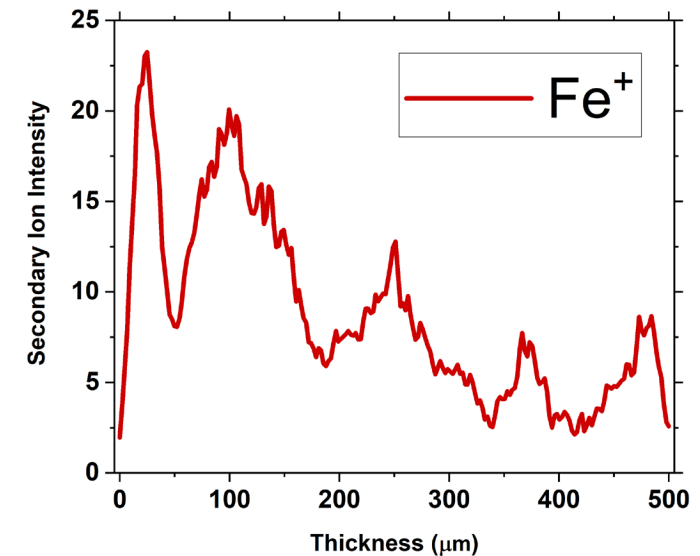
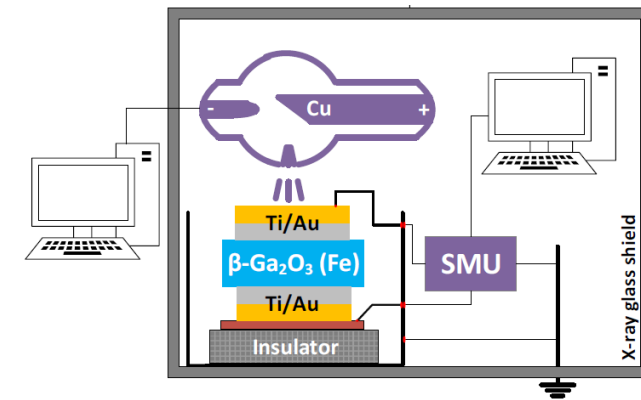
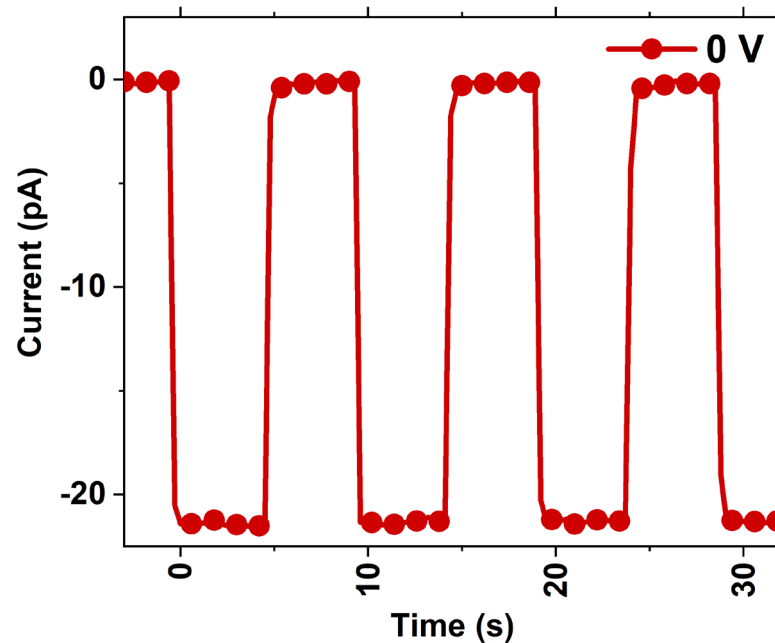
Au/Ti/ $\beta$ -Ga<sub>2</sub>O<sub>3</sub>/Ti/Au I-V characteristic curve

I. Hany et al., "Low temperature cathodoluminescence study of Fe-doped  $\beta$ -Ga<sub>2</sub>O<sub>3</sub>,"  
Materials Letters 257, 126744, 2019

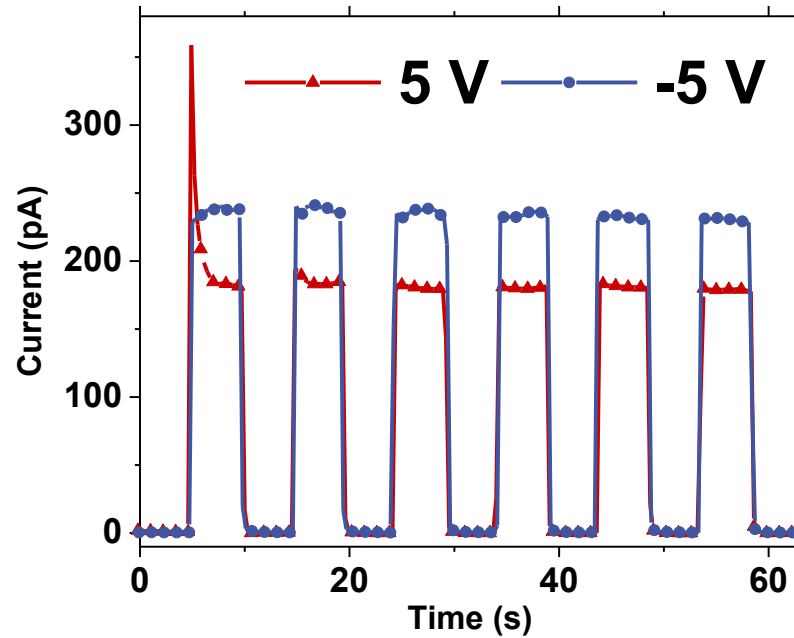
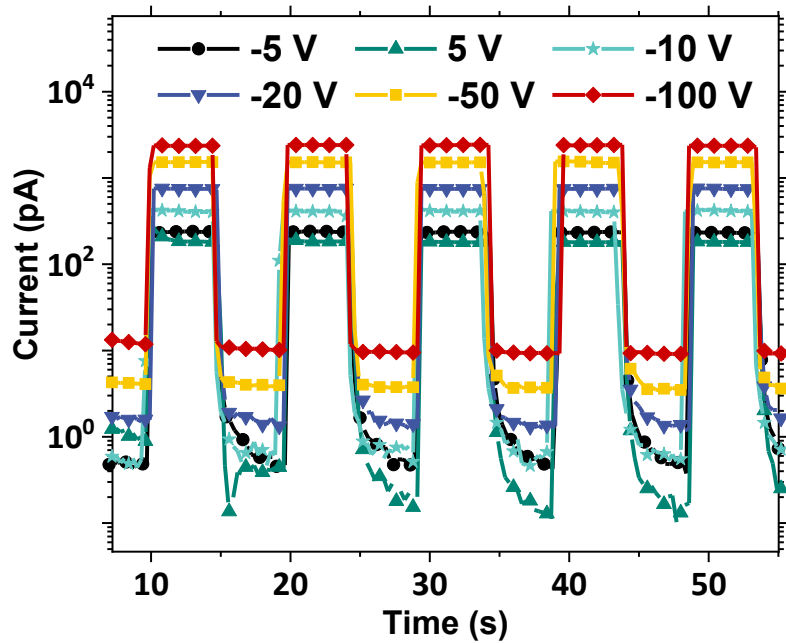
## IV. XRIC Characterization

- Zero Voltage mode (Passive operation) (45 KV, 40 mA)
  - X-ray induced current reaching -21 pA
  - Dark transient current of -0.15 (+/-0.05) pA
  - SNR = 139
  - No experimental lag

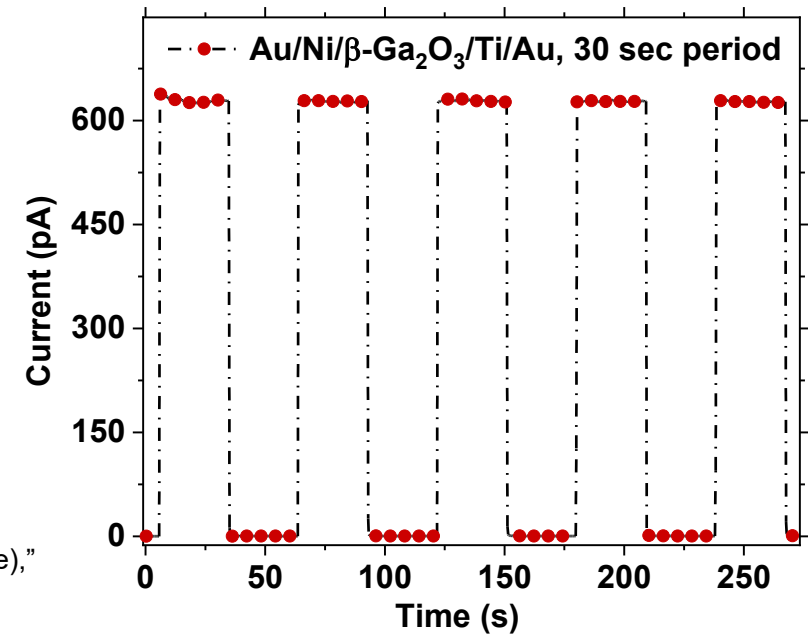
$$SNR = \frac{I_{x\text{-ray induced}} - I_{\text{dark}}}{I_{\text{dark}}}$$



# IV. XRIC Characterization

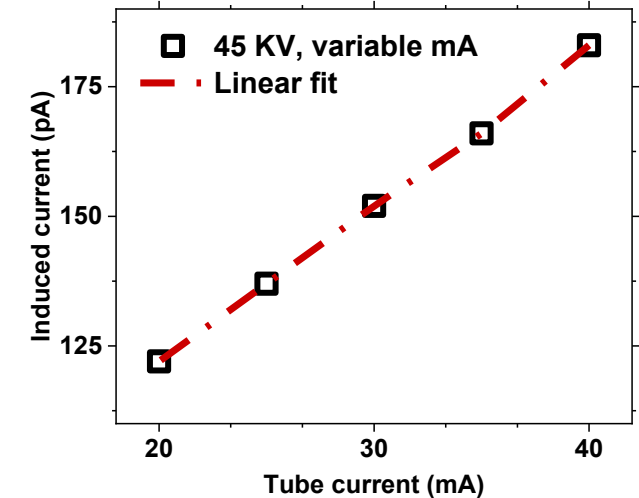
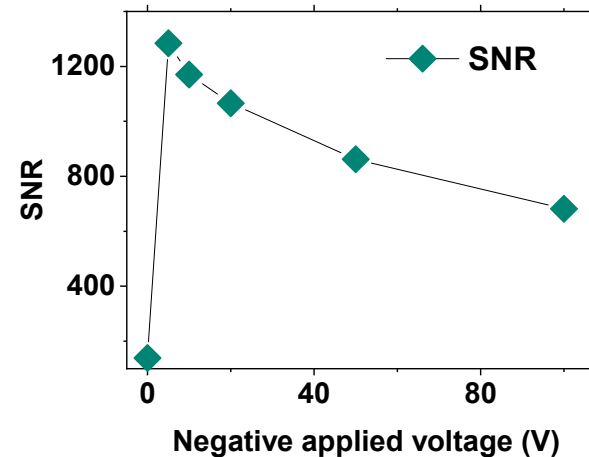
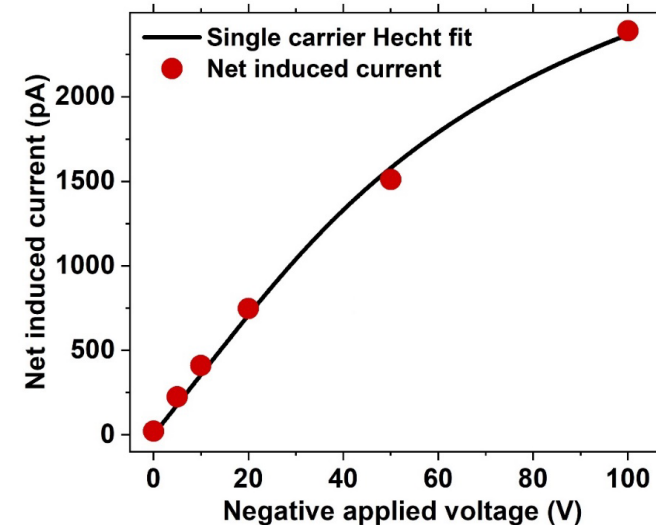


I. Hany et al., "Fast X-ray detectors based on bulk  $\beta$ -Ga<sub>2</sub>O<sub>3</sub> (Fe)," J. Mater. Sci. 55, 9461-9469, 2020.



## IV. XRIC Characterization

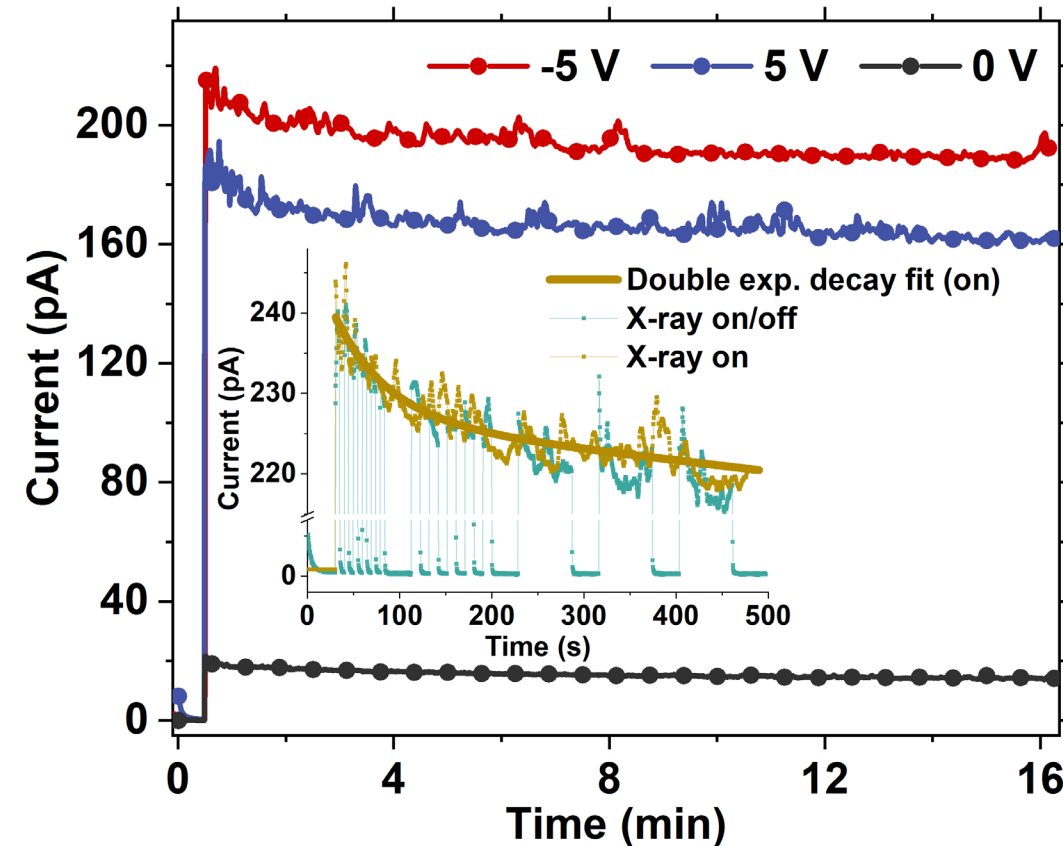
- SNR for operating voltages between -5 V and -50 V stays above 800 and decreases for the higher applied voltages.
- SNR stays above 1000 for applied voltages between -5 V and -20 V, and it is further optimized at -5 V exceeding 1200.
- $\mu\tau$  factor calculated from single carrier Hecht model treatment was  $2.28 \times 10^{-5} \text{ cm}^2/\text{V}$ 
  - 45.6  $\mu\text{m}$  carrier drift length for 10 V.
  - 456  $\mu\text{m}$  carrier drift length for 100 V.



I. Hany et al., "Fast X-ray detectors based on bulk  $\beta\text{-Ga}_2\text{O}_3(\text{Fe})$ ,"  
J. Mater. Sci. 55, 9461-9469, 2020.

## IV. XRIC Characterization

- Highly stable XRIC even at very low operating voltages (5,-5,0 V)
- Small exponential decay within the first minute that stabilizes after that
  - $\tau_1 = 57.7 \text{ sec}$  and  $\tau_2 > 10^6 \text{ sec}$ , stability
  - Less than 10% decrease in the first minute
- Operation status independent (for the ON/OFF frequency used)
  - Indicating ion migration and charge accumulation
  - Slight polarization effect



I. Hany et al., "Fast X-ray detectors based on bulk  $\beta\text{-Ga}_2\text{O}_3$  (Fe)," J. Mater. Sci. 55, 9461-9469, 2020.

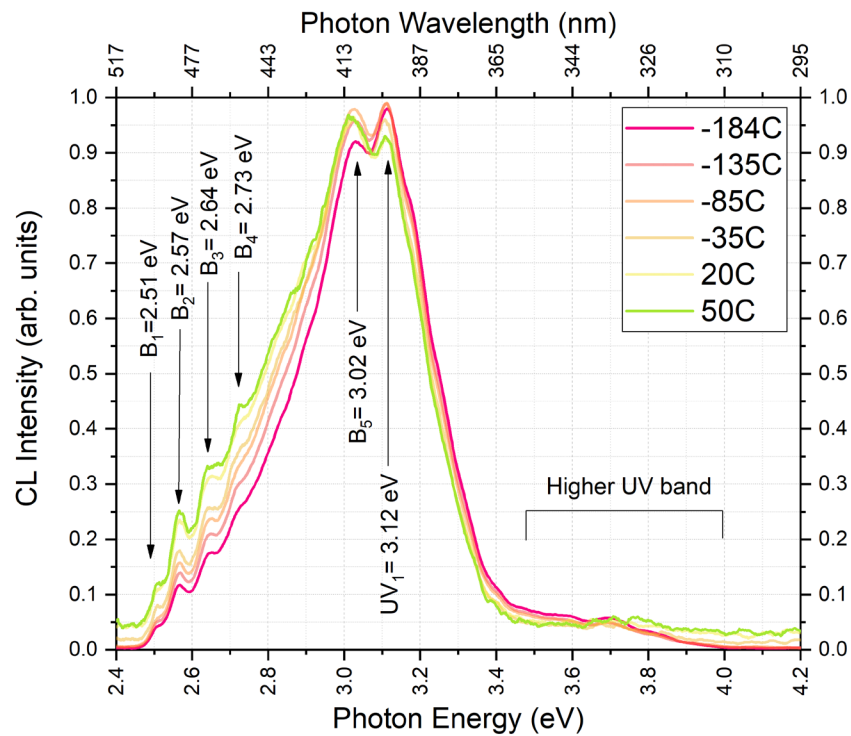
## IV. XRIC Characterization

- **a-Ga<sub>2</sub>O<sub>3</sub>**: (H. Liang et al., “Flexible X-ray Detectors Based on Amorphous Ga<sub>2</sub>O<sub>3</sub> Thin Films,” ACS Photonics, vol. 6, no. 2, pp. 351–359, 2019.)
- **Unintentionally doped β-Ga<sub>2</sub>O<sub>3</sub>**: (X. Lu et al., “Schottky x-ray detectors based on a bulk β-Ga<sub>2</sub>O<sub>3</sub> substrate,” Appl. Phys. Lett., vol. 112, no. 10, p. 103502, 2018.) and (X. Lu et al., “X-ray Detection Performance of Vertical Schottky Photodiodes Based on a Bulk β-Ga<sub>2</sub>O<sub>3</sub> Substrate Grown by an EFG Method,” ECS J. Solid State Sci. Technol., vol. 8, no. 7, pp. Q3046–Q3049, 2019.)

| Material   | Preparation method  | Rise time (s) | Decay time (s) | SNR  |
|--|---|---------------|----------------|--|
| <b>a-Ga<sub>2</sub>O<sub>3</sub></b>                       | RF sputtering (PO <sub>2</sub> 1.4 × 10 <sup>-3</sup> Pa) | 15.5          | 1.1            | -  |
|  | RF Sputtering (PO <sub>2</sub> 1.0 × 10 <sup>-3</sup> Pa) | 50.1          | 3.3            | >10 <sup>4</sup>   |
| <b>Unintentionally doped β-Ga<sub>2</sub>O<sub>3</sub></b> | EFG   | 18.3 (-15 V)  | 20.9 (-15 V)   | >800 (-15 V)   |
|  |   | <0.02 (0 V)   | <0.02 (0 V)    | -  |
| <b>β-Ga<sub>2</sub>O<sub>3</sub> (Fe)</b>                  | EFG   | <0.3          | <0.3           | >10 <sup>3</sup> (low voltages)<br>>10 <sup>2</sup> (0 V and high voltage) |

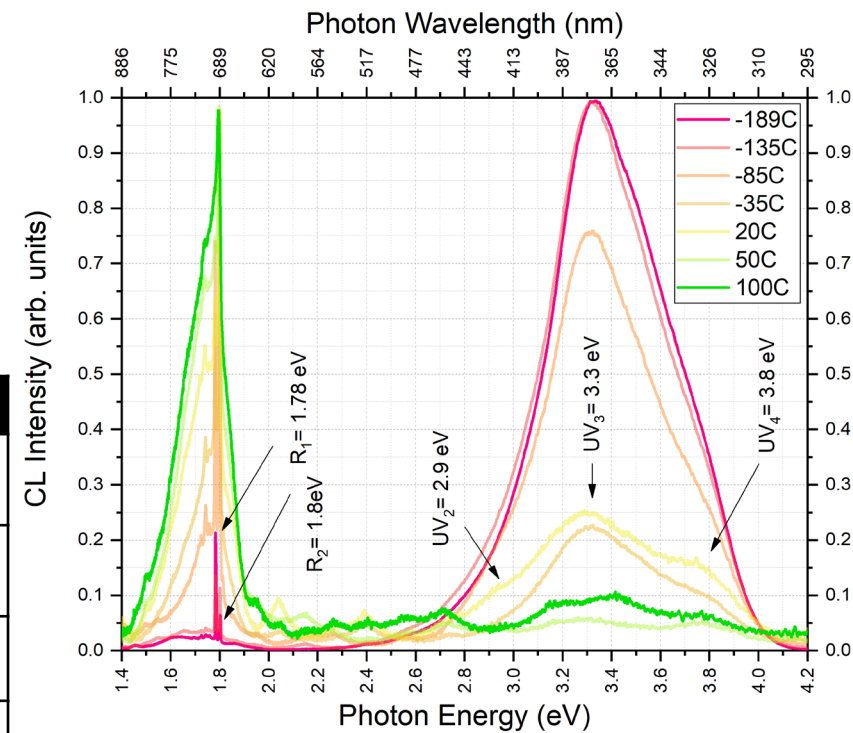
I. Hany et al., “Fast X-ray detectors based on bulk β-Ga<sub>2</sub>O<sub>3</sub> (Fe),” J. Mater. Sci. 55, 9461-9469, 2020.

# V. Temperature-dependent CL $\beta\text{-Ga}_2\text{O}_3$ (Fe)



- HT air annealing potentially decreases  $V_O$  concentration and eliminates  $V_{Ga}+V_O$  complexes.
- Potential change in  $V_{Ga}$  nature and/or concentration.
- Red luminescence possible origins are (1) Nitrogen diffusion and (2) Cr impurities. New evidence points to the latter.

| Defect       | Defect type             | Signature                    |
|--------------|-------------------------|------------------------------|
| $V_{Ga}+V_O$ | Vacancy                 | $B_{1-4}$ (acceptor)         |
| $V_O$        | Vacancy                 | $B_5$ and $UV_{1-3}$ (donor) |
| $V_{Ga}$     | Vacancy                 | $B_5$ (acceptor)             |
| $Fe_{Ga}$    | Substitutional (dopant) | $UV_1$ (acceptor)            |
| STH          | Electronic defect       | $UV_{2-4}$                   |



I. Hany et al., "Low temperature cathodoluminescence study of Fe-doped  $\beta\text{-Ga}_2\text{O}_3$ ," Materials Letters 257, 126744, 2019.

## VI. Summary

- $\beta\text{-Ga}_2\text{O}_3(\text{Fe})$  was investigated as a direct X-ray detection material motivated by its high resistivity and ultra-low leakage current.
  - High SNR under three operation modes
  - High linearity between X-ray induced photocurrent and X-ray tube current
  - Improved transport properties
    - Controlling Fe and Cr distribution may increase  $\mu\tau$ -factor
  - High stability upon continuous illumination for 15 minutes.
    - $V_{\text{O}}$  and  $V_{\text{Ga}}$  potentially assist in the initial polarization effect
- The results demonstrate the great potential of  $\beta\text{-Ga}_2\text{O}_3(\text{Fe})$  as a radiation resistant X-ray detector with excellent temporal response for a wide range of applications.



**Thank you for your attention!**